

Collective properties of nucleus-nucleus collisions from AGS to LHC energies

V P Konchakovski¹, V D Toneev², W Cassing¹, E L Bratkovskaya³,
S A Voloshin⁴ and V Voronyuk⁵

¹ Institute for Theoretical Physics, University of Giessen, Giessen, Germany

² Joint Institute for Nuclear Research, Dubna, Russia

³ Institute for Theoretical Physics, University of Frankfurt, Frankfurt, Germany

⁴ Wayne State University, Detroit, Michigan, USA

⁵ Bogolyubov Institute for Theoretical Physics, Kiev, Ukraine

E-mail: Wolfgang.Cassing@theo.physik.uni-giessen.de

Abstract. The azimuthal anisotropies of the collective transverse flow of charged hadrons are investigated in a wide range of heavy-ion collision energies within the microscopic Parton-Hadron-String Dynamics (PHSD) transport approach which incorporates explicit partonic degrees-of-freedom in terms of strongly interacting quasiparticles (quarks and gluons) in line with an equation-of-state from lattice QCD as well as the dynamical hadronization and hadronic collision dynamics in the final reaction phase. The experimentally observed increase of the elliptic flow v_2 of charged hadrons with collision energy is successfully described in terms of the PHSD approach. The analysis of higher-order harmonics v_3 and v_4 in the azimuthal angular distribution shows a similar tendency of growing deviations between partonic and purely hadronic models with increasing collision energy. This demonstrates that the excitation functions of azimuthal anisotropies reflect the increasing role of quark-gluon degrees of freedom in the early phase of relativistic heavy-ion collisions. Furthermore, the specific variation of the ratio $v_4/(v_2)^2$ with respect to bombarding energy, centrality and transverse momentum is found to provide valuable information on the underlying partonic dynamics.

1. Introduction

The discovery of large azimuthal anisotropic flow at the Relativistic-Heavy-Ion-Collider (RHIC) provides a conclusive evidence for the creation of dense partonic matter in ultra-relativistic nucleus-nucleus collisions. With sufficiently strong parton interactions, the medium in the collision zone can be expected to achieve local equilibrium and exhibit approximately hydrodynamic flow [1, 2, 3]. The momentum anisotropy is generated due to pressure gradients of the initial “almond-shaped” collision zone produced in noncentral collisions [1, 2]. The azimuthal pressure gradient extinguishes itself soon after the start of the hydrodynamic evolution, so the final flow is only weakly sensitive to later stages of the fireball evolution. The pressure gradients have to be large enough to translate an early asymmetry in density of the initial state to a final-state momentum-space anisotropy. In these collisions a new state of strongly interacting matter is created, being characterized by a very low shear viscosity η to entropy density s ratio, η/s , close to a nearly perfect fluid [4, 5, 6]. Lattice QCD (lQCD) calculations [7, 8, 9] indicate that a crossover region between hadron and quark-gluon matter should have been reached in these experiments.

An experimental manifestation of this collective flow is the anisotropic emission of charged particles in the plane transverse to the beam direction. This anisotropy is described by the different flow parameters defined as the proper Fourier coefficients v_n of the particle distributions in azimuthal angle ψ with respect to the reaction plane angle Ψ_{RP} . At the highest RHIC collision energy of $\sqrt{s_{NN}} = 200$ GeV, differential elliptic flow measurements $v_2(p_T)$ have been reported for a broad range of centralities or number of participants N_{part} . For N_{part} estimates, the geometric fluctuations associated with the positions of the nucleons in the collision zone serve as the underlying origin of the initial eccentricity fluctuations. These data are found to be in accord with model calculations that an essentially locally equilibrated quark gluon plasma (QGP) has little or no viscosity [10, 11, 12]. Collective flow continues to play a central role in characterizing the transport properties of the strongly interacting matter produced in heavy-ion collisions at RHIC. Particle anisotropy measurements are considered as key observables for a reliable extraction of transport coefficients.

It was shown before that higher-order anisotropy harmonics, in particular v_4 , may provide a more sensitive constraint on the magnitude of η/s and the freeze-out dynamics, and the ratio $v_4/(v_2)^2$ might indicate whether a full local equilibrium is achieved in the QGP [13]. The role of fluctuations and so-called ‘nonflow’ correlations are important for such measurements. It is well established that initial eccentricity fluctuations significantly influence the magnitudes of $v_{2,4}$ [14, 15]. However, the precise role of nonflow correlations, which lead to a systematic error in the determination of $v_{2,4}$, is less clear. Recently, significant attention has been given to the study of the influence of initial geometry fluctuations on higher order eccentricities $\epsilon_n(n \geq 3)$ for a better understanding of how such fluctuations manifest themselves in the harmonic flow correlations characterized by v_n . Even more, it was proposed that the analysis of v_n^2 for all values of n can be considered as an analogous measurement to the Power Spectrum extracted from the Cosmic Microwave Background Radiation providing a possibility to observe superhorizon fluctuations [16].

A large number of anisotropic flow measurements have been performed by many experimental groups at SIS, AGS, SPS and RHIC energies over the last twenty years. Very recently, the azimuthal asymmetry has been measured also at the LHC [17]. However, the fact that these data have not been obtained under the same experimental conditions as at RHIC experiments, does not directly allow for a detailed and meaningful comparison in most cases. The experimental differences include: different centrality selection, different transverse momentum acceptance, different particle species, different rapidity coverage and different methods for flow analysis as pointed out in Ref. [18].

The Beam-Energy-Scan (BES) program proposed at RHIC [19] covers the energy interval from $\sqrt{s_{NN}} = 200$ GeV, where partonic degrees of freedom play a decisive role, down to the AGS energy of $\sqrt{s_{NN}} \approx 5$ GeV, where most experimental data may be described successfully in terms of hadronic degrees-of-freedom, only. Lowering the RHIC collision energy and studying the energy dependence of anisotropic flow allows to search for the possible onset of the transition to a phase with partonic degrees-of-freedom at an early stage of the collision as well as possibly to identify the location of the critical end-point that terminates the cross-over transition at small quark-chemical potential to a first order phase transition at higher quark-chemical potential [20, 21].

This contribution aims to summarize excitation functions for different harmonics of the charged particle anisotropy in the azimuthal angle at midrapidity in a wide transient energy range, *i.e.* from the AGS to the top RHIC energy. The first attempts to explain the preliminary STAR data with respect to the observed increase of the elliptic flow v_2 with the collision energy have failed since the traditional available models did not allow to clarify the role of the partonic phase [22]. In this contribution we investigate the energy behavior of different flow coefficients, their scaling properties and differential distributions (cf. Ref. [23, 24]). Our analysis of the

STAR/PHENIX RHIC data – based on recent results of the BES program – will be performed within the Parton-Hadron-String Dynamics (PHSD) transport model [25] that includes explicit partonic degrees-of-freedom as well as a dynamical hadronization scheme for the transition from partonic to hadronic degrees-of-freedom and vice versa. For more detailed descriptions of PHSD and its ingredients we refer the reader to Refs. [26, 27, 28, 29].

2. Results for collective flows

We directly continue with the results from PHSD in comparison with other approaches and the available experimental data.

2.1. Elliptic flow

The largest component, known as elliptic flow v_2 , is one of the early observations at RHIC [30]. The elliptic flow coefficient is a widely used quantity characterizing the azimuthal anisotropy of emitted particles,

$$v_2 = \langle \cos(2\psi - 2\Psi) \rangle = \left\langle \frac{p_x^2 - p_y^2}{p_x^2 + p_y^2} \right\rangle, \quad (1)$$

where Ψ_{RP} is the azimuth of the reaction plane, p_x and p_y are the x and y component of the particle momenta and the brackets denote averaging over particles and events. This coefficient can be considered as a function of centrality, pseudorapidity η and/or transverse momentum p_T . We note that the reaction plane in PHSD is given by the $(x - z)$ plane with the z -axis in beam direction. The reaction plane is defined as a plane containing the beam axes and the impact parameter vector.

We recall that at high bombarding energies the longitudinal size of the Lorentz contracted nuclei becomes negligible compared to its transverse size. The forward shadowing effect then becomes negligible and the elliptic flow fully develops in-plane, leading to a positive value of the average flow v_2 since no shadowing from spectators takes place. In Fig. 1 (l.h.s.) the experimental v_2 data compilation for the transient energy range is compared to the results from HSD calculations and further available model results as included in Ref. [22]. The centrality selection is the same for the data and the various models.

In order to interpret the results in Fig. 1 we have to recall the various ingredients of the models employed for comparison. The UrQMD (Ultra relativistic Quantum Molecular Dynamics) model is a microscopic transport theory based on the relativistic Boltzmann equation [31, 32]. It allows for the on-shell propagation of all hadrons along classical trajectories in combination with stochastic binary scattering, color string formation and resonance decay. The model incorporates baryon-baryon, meson-baryon and meson-meson interactions based on experimental data (when possible). This Boltzmann-like hadronic transport model has been employed for proton-nucleus and nucleus-nucleus collisions from AGS to RHIC energies [32]. The comparison of the data on v_2 to those from the UrQMD model will thus essentially provide information on the contribution from the hadronic phase. As seen in Fig. 1, being in agreement with data at the lowest energy $\sqrt{s_{NN}} = 9.2$ GeV, the UrQMD model results then either remain approximately constant or decrease slightly with increasing $\sqrt{s_{NN}}$; UrQMD thus does not reproduce the rise of v_2 with the collision energy as seen experimentally.

The HSD model [33, 34, 35] is also a hadron-string model including formally the same processes as UrQMD. However, being based on the off-shell generalized transport equation [29] followed from Kadanoff-Baym approach, the quasiparticles in the HSD model take into account in-medium modifications of their properties in the nuclear environment which is rather essential for many observables and in particular for dileptons. Detailed comparisons between HSD and UrQMD for central Au+Au (Pb+Pb) collisions have been reported in Ref. [36] from AGS to top SPS energies with respect to a large experimental data set. Indeed, both hadronic approaches

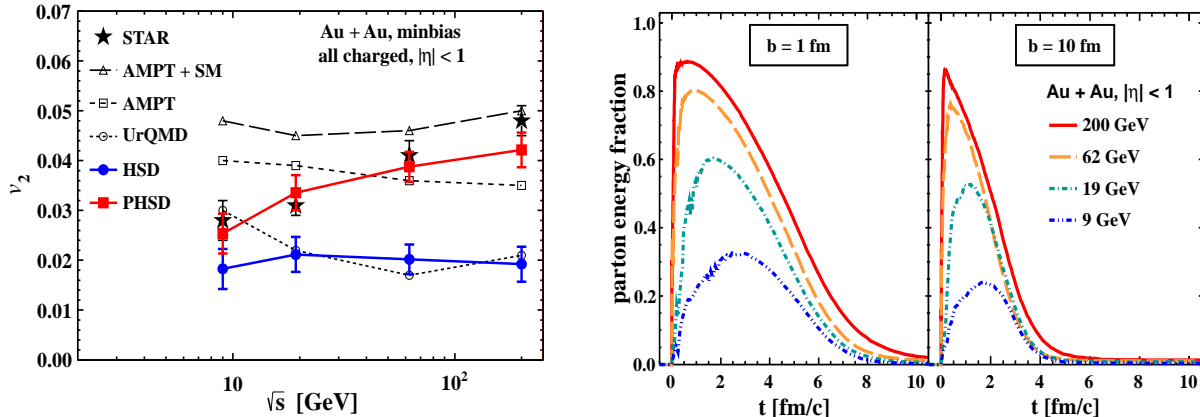


Figure 1. (l.h.s.) The average elliptic flow v_2 of charged particles at midrapidity for minimum bias collisions at $\sqrt{s_{NN}} = 9.2, 19.6, 62.4$ and 200 GeV (stars is taken from the data compilation of Ref. [22]). The corresponding results from different models are compared to the data and explained in more detail in the text. (r.h.s.) Evolution of the parton fraction of the total energy density at midrapidity (from PHSD) for different collision energies at impact parameters $b = 1$ fm and 10 fm.

yield similar results on the level of 20-30% which is also the maximum deviation from the data sets. Accordingly, the HSD model also predicts an approximately energy-independent flow v_2 in quite close agreement with the UrQMD results. We may thus conclude that the rise of v_2 with bombarding energy is not do to hadronic interactions and models with partonic degrees-of-freedom have to be addressed.

The AMPT (A Multi Phase Transport model) [37, 38] uses initial conditions of a perturbative QCD (pQCD) inspired model which produces multiple minijet partons according to the number of binary initial nucleon-nucleon collisions. These (massless) minijet partons undergo scattering (without potentials) before they are allowed to fragment into hadrons. The string melting (SM) version of the AMPT model (labeled in Fig. 1 as AMPT-SM) is based on the idea that the existence of strings (or hadrons) is impossible for energy densities beyond a critical value of $\varepsilon \sim 1$ GeV/fm³. Hence they melt the strings to (massless) partons. This is done by converting the mesons to a quark and anti-quark pair, baryons to three quarks *etc.* fulfilling energy-momentum conservation. The subsequent scattering of the quarks are based on a parton cascade with (adjustable) effective cross sections which are significantly larger than those from pQCD [37, 38]. Once the partonic interactions terminate, the partons hadronize through the mechanism of parton coalescence.

We find from Fig. 1 that the interactions between the minijet partons in the AMPT model indeed increase the elliptic flow significantly as compared to the hadronic models UrQMD and HSD. An additional inclusion of interactions between partons in the AMPT-SM model gives rise to another 20% of v_2 bringing it into agreement (for AMPT-SM) with the data at the maximal collision energy. So, both versions of the AMPT model indicate the importance of partonic contributions to the observed elliptic flow v_2 but do not reproduce its growth with $\sqrt{s_{NN}}$. The authors address this result to the partonic-equation-of state (EoS) employed which corresponds to a massless and noninteracting relativistic gas of particles. This EoS deviates severely from the results of lattice QCD calculations for temperatures below $2-3 T_c$. Accordingly, the degrees-of-freedom are propagated without self-energies and a parton spectral function.

The PHSD approach incorporates the latter medium effects in line with a lQCD equation-of-

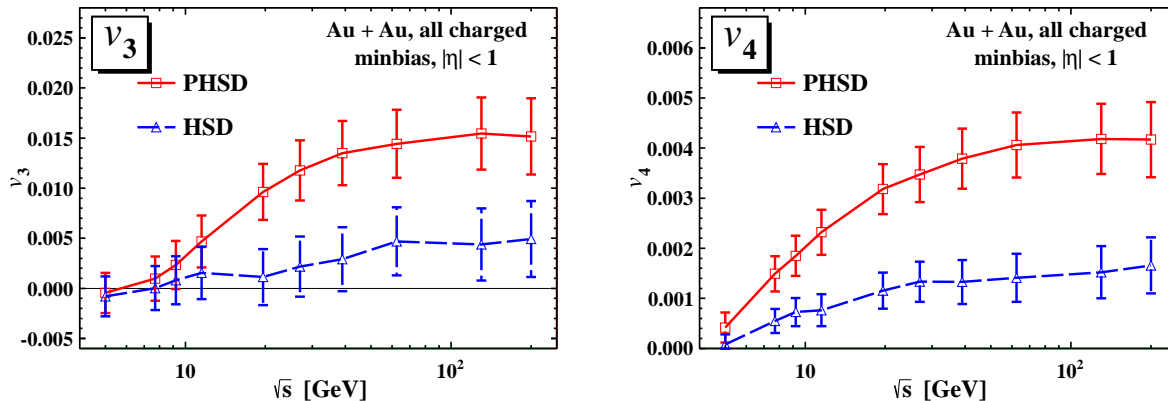


Figure 2. Average anisotropic flows v_3 (l.h.s.) and v_4 (r.h.s.) of charged particles at mid-pseudorapidity for minimum bias Au + Au collisions calculated within the PHSD (solid lines, red) and HSD (dashed lines, blue) models.

state and also includes a dynamical hadronization scheme based on covariant transition rates. As has been demonstrated in Refs. [23, 24] and explicitly shown in Fig. 1 (l.h.s.), the elliptic flow v_2 from PHSD (red line) agrees with the data from the STAR collaboration and clearly shows an increase with bombarding energy. Note that PHSD and AMPT-SM practically give the same elliptic flow at the top RHIC energy of $\sqrt{s_{NN}} = 200$ GeV.

An explanation for the increase in v_2 with collision energy is provided in Fig. 1 (r.h.s.). Here we show the partonic fraction of the energy density with respect to the total energy where the energy densities are calculated at mid-rapidity. As discussed above the main contribution to the elliptic flow is coming from an initial partonic stage at high \sqrt{s} . The fusion of partons to hadrons or, inversely, the melting of hadrons to partonic quasiparticles occurs when the local energy density is about $\varepsilon \approx 0.5$ GeV/fm³. As follows from Fig. 1, the parton fraction of the total energy goes down substantially with decreasing bombarding energy while the duration of the partonic phase is roughly the same. The maximal fraction reached is the same in central and peripheral collisions but the parton evolution time is shorter in peripheral collisions. One should recall again the important role of the repulsive mean-field for partons in the PHSD model that leads to an increase of the flow v_2 with respect to HSD predictions (cf. also Ref. [39]). We point out in addition that the increase of v_2 in PHSD relative to HSD is also partly due to the higher interaction rates in the partonic medium because of a lower ratio of η/s for partonic degrees-of-freedom at energy densities above the critical energy density than for hadronic media below the critical energy density [40, 41]. The relative increase in v_3 and v_4 in PHSD essentially is due to the higher partonic interaction rate and thus to a lower ratio η/s in the partonic medium which is mandatory to convert initial spacial anisotropies to final anisotropies in momentum space [42].

2.2. Higher-order flow harmonics

Depending on the location of the participant nucleons in the nucleus at the time of the collision, the actual shape of the overlap area may vary: the orientation and eccentricity of the ellipse defined by the participants fluctuates from event to event. Note, however, that by averaging over many events an almond shape is regained for the same impact parameter.

Recent studies suggest that fluctuations in the initial state geometry can generate higher-order flow components [10, 16, 43, 44]. The azimuthal momentum distribution of the emitted

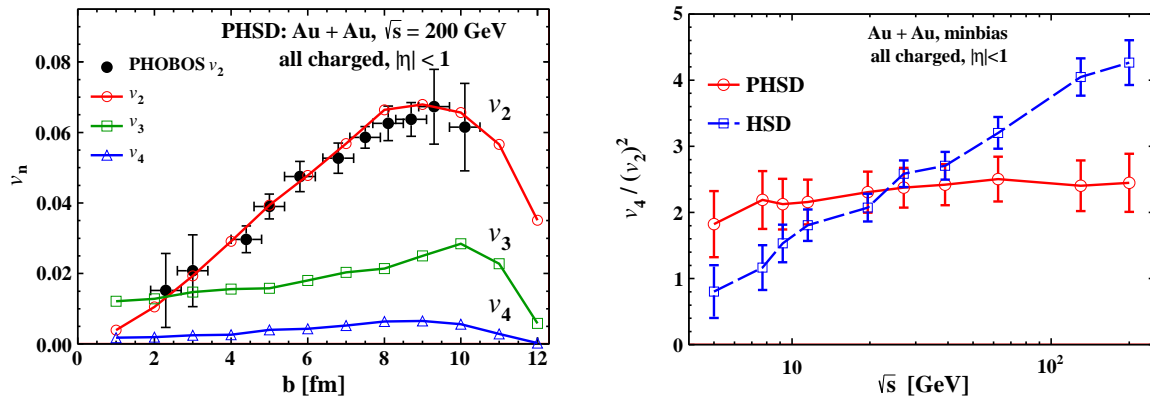


Figure 3. (l.h.s.) Impact parameter dependence of anisotropic flows of charged particles at mid-pseudorapidity for minimum bias collisions of Au+Au at $\sqrt{s_{NN}} = 200$ GeV. Experimental points are from Ref. [48]. (r.h.s.) Beam energy dependence of the ratio $v_4/(v_2)^2$ for Au+Au collisions. The solid and dashed curves are calculated within the PHSD and HSD models, respectively.

particles is commonly expressed in the form of Fourier series as

$$E \frac{d^3 N}{d^3 p} = \frac{d^2 N}{2\pi p_T dp_T dy} \left(1 + \sum_{n=1}^{\infty} 2v_n(p_T) \cos(n(\psi - \Psi_n)) \right), \quad (2)$$

where v_n is the magnitude of the n -th order harmonic term relative to the angle of the initial-state spatial plane of symmetry Ψ_n . The anisotropy in the azimuthal angle ψ is usually characterized by the even order Fourier coefficients with the reaction plane $\Psi_n = \Psi_{RP}$: $v_n = \langle \exp(in(\psi - \Psi_{RP})) \rangle$ ($n = 2, 4, \dots$), since for a smooth angular profile the odd harmonics vanish. For the odd components, e.g. v_3 , one should take into account event-by-event fluctuations with respect to the participant plane $\Psi_n = \Psi_{PP}$. We calculate the v_3 coefficients with respect to Ψ_3 as: $v_3\{\Psi_3\} = \langle \cos(3[\psi - \Psi_3]) \rangle / Res(\Psi_3)$. The event plane angle Ψ_3 and its resolution $Res(\Psi_3)$ are calculated as described in Ref. [45] via the two-sub-events method [46, 47].

In Fig. 2 we display the PHSD and HSD results for the anisotropic flows v_3 and v_4 of charged particles at mid-pseudorapidity for Au+Au collisions as a function of $\sqrt{s_{NN}}$. The pure hadronic model HSD gives $v_3 \approx 0$ for all energies. Accordingly, the results from PHSD (dashed red line) are systematically larger than from HSD (dashed blue line). Unfortunately, our statistics are not good enough to allow for more precise conclusions. The hexadecupole flow v_4 stays almost constant in the energy range $\sqrt{s_{NN}} \geq 10$ GeV; at the same time the PHSD gives noticeably higher values than HSD which we attribute to the higher interaction rate in the partonic phase, i.e. a lower ratio of η/s in the partonic phase [40, 41].

Alongside with the integrated flow coefficients v_n the PHSD model reasonably describes their distribution over centrality or impact parameter b . A specific comparison at $\sqrt{s_{NN}} = 200$ GeV is shown in Fig. 3 for v_2, v_3 and v_4 . While v_2 increases strongly with b up to peripheral collisions, v_3 and v_4 are only weakly sensitive to the impact parameter. The triangular flow is always somewhat higher than the hexadecupole flow in the whole range of impact parameters b .

2.3. Ratios of different harmonics

Different harmonics can be related to each other. In particular, hydrodynamics predicts that $v_4 \propto (v_2)^2$ [49]. The simplest prediction that $v_4 = 0.5(v_2)^2$ is given for a boosted thermal freeze-out distribution of an ideal fluid, Ref. [50]. In this work it was noted also that v_4 is largely

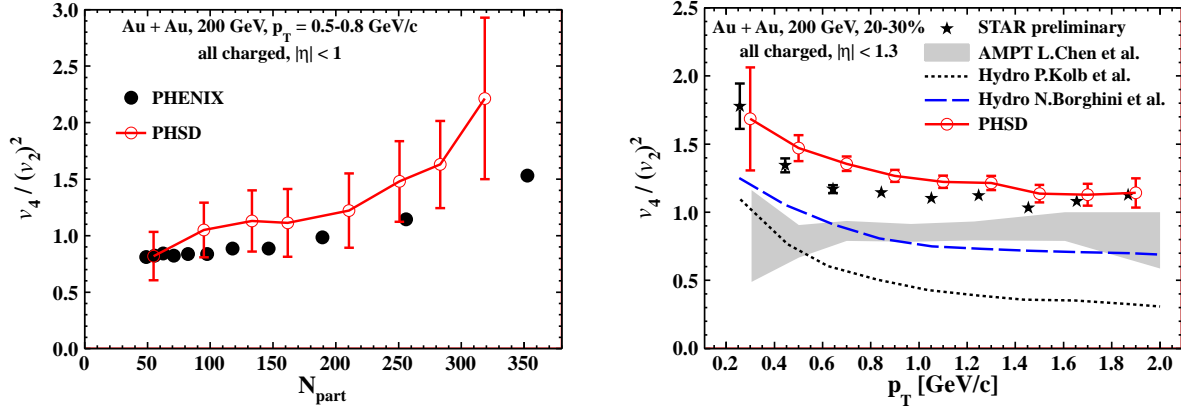


Figure 4. (l.h.s.) Participant number dependence of the $v_4/(v_2)^2$ ratio of charged particles for Au+Au ($\sqrt{s_{NN}} = 200$ GeV) collisions. The experimental data points for $0.5 < p_T < 0.8$ GeV/c are from Ref. [51].

(r.h.s.) Transverse momentum dependence of the ratio $v_4/(v_2)^2$ of charged particles for Au+Au (at $\sqrt{s_{NN}} = 200$ GeV) collisions. The dashed and dot-dashed lines are calculated within the hydrodynamic approaches from Refs. [49] and [50], respectively. The shaded region corresponds to the results from the AMPT model [53]. The experimental data points are from the STAR Collaboration [52].

generated by an intrinsic elliptic flow (at least at high p_T) rather than the fourth order moment of the fluid flow. This is a motivation for studying the ratio $v_4/(v_2)^2$ rather than v_4 alone. As is seen in Fig. 4 (r.h.s.), indeed the ratio calculated within the PHSD model is practically constant in the whole range of $\sqrt{s_{NN}}$ considered but significantly deviates from the ideal fluid estimate of 0.5. In contrast, neglecting dynamical quark-gluon degrees-of-freedom in the HSD model, we obtain a monotonous growth of this ratio.

The dependence of the $v_4/(v_2)^2$ ratio versus the number of participants N_{part} is shown in Fig. 4 for charged particles produced in Au + Au collisions at $\sqrt{s_{NN}} = 200$ GeV. The PHSD results are roughly in agreement with the experimental data points from Ref. [52] but overshoot them for $N_{part} \sim 250$.

As pointed out before, the ratio $v_4/(v_2)^2$ is sensitive to the microscopic dynamics. In this respect we show the transverse momentum dependence of the ratio $v_4/(v_2)^2$ in Fig. 4 for charged particles produced in Au+Au collisions at $\sqrt{s_{NN}} = 200$ GeV (20-30% centrality). The PHSD results are quite close to the experimental data points from Ref. [52], however, overestimate the measurements by up to 20%. The hydrodynamic results – plotted in the same figure – significantly underestimate the experimental data and noticeably depend on viscosity. The partonic AMPT model [53] discussed above also predicts a slightly lower ratio than the measured one, however, being in agreement with both hydrodynamic models for $p_T > 0.8$ GeV/c. Our interpretation of Fig. 4 (r.h.s.) is as follows: the data are not compatible with ideal hydrodynamics and a finite shear viscosity is mandatory (in viscous hydrodynamics) to come closer the experimental observations. The kinetic approaches AMPT and PHSD perform better but either overestimate (in AMPT) or slightly underestimate the scattering rate of soft particles (in PHSD). An explicit study of the centrality dependence of these ratios should provide further valuable information.

3. Conclusions

In summary, relativistic collisions of Au+Au from $\sqrt{s_{NN}} = 5$ to 200 GeV have been studied within the PHSD approach which includes the dynamics of explicit partonic degrees-of-freedom as well as dynamical local transition rates from partons to hadrons and also the final hadronic scatterings. Whereas earlier studies have been carried out for longitudinal rapidity distributions of various hadrons, their transverse mass spectra and the elliptic flow v_2 as compared to available data at SPS and RHIC energies [25, 26], here we have focussed on the PHSD results for the collective flow coefficients v_2, v_3 and v_4 in comparison to recent experimental data in the large energy range from the RHIC Beam-Energy-Scan (BES) program as well as different theoretical approaches ranging from hadronic transport models to ideal and viscous hydrodynamics. We mention explicitly that the PHSD model from Ref. [26] has been used for all calculations performed in this study and no tuning (or change) of model parameters has been performed.

We have found that the anisotropic flows – elliptic v_2 , triangular v_3 , hexadecapole v_4 – are reasonably described within the PHSD model in the whole transient energy range naturally connecting the hadronic processes at lower energies with ultrarelativistic collisions where the quark-gluon degrees of freedom become dominant. The smooth growth of the elliptic flow v_2 with the collision energy demonstrates the increasing importance of partonic degrees of freedom. This feature is reproduced by neither hadron-string based kinetic models nor A Multi Phase Transport (AMPT) model treating the partonic phase in a simplified manner. Other signatures of the transverse collective flow, the higher-order harmonics of the transverse anisotropy v_3 and v_4 change only weakly from $\sqrt{s_{NN}} \sim 7$ GeV to the top RHIC energy of $\sqrt{s_{NN}} = 200$ GeV, roughly in agreement with experiment. As shown in this study, this success is related to a consistent treatment of the interacting partonic phase in PHSD whose fraction increases with the collision energy.

The analysis of correlations between particles emitted in ultrarelativistic heavy-ion collisions at large relative rapidity has revealed an azimuthal structure that can be interpreted as solely due to collective flow [54, 55, 56, 57]. This interesting new phenomenon, denoted as triangular flow, results from initial state fluctuations and a subsequent hydrodynamic-like evolution. Unlike the usual directed flow, this phenomenon has no correlation with the reaction plane and should depend weakly on rapidity. Event-by-event hydrodynamics [58] has been a natural framework for studying this triangular collective flow but it has been of interest also to investigate these correlations in terms of the PHSD model. We have found the third harmonics to increase steadily in PHSD with bombarding energy. The coefficient v_3 is compatible with zero for $\sqrt{s_{NN}} > 20$ GeV in case of the hadronic transport model HSD which does not develop ‘ridge-like’ correlations. In this energy range PHSD gives a positive v_3 due to dominant partonic interactions.

Different harmonics can be related to each other and in particular, hydrodynamics predicts that $v_4 \propto (v_2)^2$ [49]. In this work it was noted also that v_4 is largely generated by an intrinsic elliptic flow (at least at high p_T) rather than the fourth order moment of the fluid flow. Indeed, the ratio $v_4/(v_2)^2$ calculated within the PHSD model is approximately constant in the whole considered range of $\sqrt{s_{NN}}$ but significantly deviates from the ideal fluid estimate of 0.5. In contrast, neglecting dynamical quark-gluon degrees-of-freedom in the HSD model, we obtain a monotonous growth of this ratio.

The transverse momentum dependence of the ratio $v_4/(v_2)^2$ at the top RHIC energy has given further interesting information (*cf.* Fig. 4) by comparing the various model results to the data from STAR which are interpreted as follows: the STAR data are not compatible with ideal hydrodynamics and a finite shear viscosity is mandatory (in viscous hydrodynamics) to come closer the experimental ratio observed. The kinetic approaches AMPT and PHSD perform better but either overestimate (in AMPT) or slightly underestimate the scattering rate of soft particles (in PHSD). Our findings at LHC energies are close to those at top RHIC energy.

References

- [1] Ollitrault J Y 1992 *Phys. Rev. D* **46** 229
- [2] Heinz U and Kolb P 2002 *Nucl. Phys. A* **702** 269
- [3] Shuryak E V 2009 *Prog. Part. Nucl. Phys.* **62** 48
- [4] Shuryak E V 2005 *Nucl. Phys. A* **750** 64
- [5] Gyulassy M and McLerran L 2005 *Nucl. Phys. A* **750** 30
- [6] Peshier A and Cassing W 2005 *Phys. Rev. Lett.* **94** 172301
- [7] Aoki Y *et al.* 2006 *Nature* **443** 675
- [8] Aoki Y *et al.* 2006 *Phys. Lett. B* **643** 46
- [9] Borsanyi S *et al.* 2010 *JHEP* **1009** 073
- [10] Adare A *et al.* 2007 *Phys. Rev. Lett.* **98** 172301
- [11] Romatschke P and Romatschke U 2007 *Phys. Rev. Lett.* **99** 172301
- [12] Xu Z, Greiner C and Stöcker H 2008 *Phys. Rev. Lett.* **101** 082302
- [13] Bhalerao R S *et al.* 2005 *Phys. Lett. B* **627** 49
- [14] Hama Y *et al.* 2008 *Phys. Atom. Nucl.* **71** 1558
- [15] Alver B *et al.* 2007 *Phys. Rev. Lett.* **98** 242302
- [16] Mishra A P *et al.* 2008 *Phys. Rev. C* **77** 064902
- [17] Aamodt K *et al.* 2010 *Phys. Rev. Lett.* **105** 252302
- [18] Taranenko A 2011 *arXiv:1101.5069*
- [19] Abelev B I *et al.* 2010 *Phys. Rev. C* **81** 024911
- [20] Lacey R A *et al.* 2007 *Phys. Rev. Lett.* **98** 092301
- [21] Aggarwal M M *et al.* 2010 *arXiv:1007.2613*
- [22] Nasim M, Kumar L, Netrakanti P K and Mohanty B 2010 *Phys. Rev. C* **82** 054908
- [23] Konchakovski V P *et al.* 2012 *Phys. Rev. C* **85** 011902
- [24] Konchakovski V P *et al.* 2012 *Phys. Rev. C* **85** 044922
- [25] Cassing W and Bratkovskaya E L 2009 *Nucl. Phys. A* **831** 215
- [26] Bratkovskaya E L, Cassing W, Konchakovski V P and Linnyk O 2011 *Nucl. Phys. A* **856** 162
- [27] Cassing W 2007 *Nucl. Phys. A* **791** 365
- [28] Cassing W 2007 *Nucl. Phys. A* **795** 70
- [29] Cassing W 2009 *Eur. J. Phys.* **168** 3
- [30] Ackermann K H *et al.* 2001 *Phys. Rev. Lett.* **86** 402
- [31] Cassing W *et al.* 1990 *Phys. Rep.* **188** 363
- [32] Bass S A *et al.* 1998 *Prog. Part. Nucl. Phys.* **41** 255
- [33] Bratkovskaya E L, Cassing W and Stöcker H 2003 *Phys. Rev. C* **67** 054905
- [34] Ehehalt W and Cassing W 1996 *Nucl. Phys. A* **602** 449
- [35] Cassing W and Bratkovskaya E L 1999 *Phys. Rep.* **308** 65
- [36] Bratkovskaya E L *et al.* 2004 *Phys. Rev. C* **69** 054907
- [37] Lin Z W and Ko C M 2002 *Phys. Rev. C* **65** 034904
- [38] Lin Z W, Ko C M, Li, B A Zhang B and Pal S 2005 *Phys. Rev. C* **72** 064901
- [39] Cassing W and Bratkovskaya E L 2008 *Phys. Rev. C* **78** 034919
- [40] Mattiello S and Cassing W 2010 *Eur. Phys. J. C* **70** 243
- [41] Demir N and Bass S A 2009 *Phys. Rev. Lett.* **102** 172302
- [42] Petersen H, Coleman-Smith C, Bass S A and Wolpert R 2011 *J. Phys. G* **38** 045102
- [43] Petersen H and Bleicher M 2010 *Phys. Rev. C* **81** 044906
- [44] Alver B and Roland G 2010 *Phys. Rev. C* **81** 054905
- [45] Adare A *et al.* 2011 *Phys. Rev. Lett.* **107** 252301
- [46] Poskanzer A M and Voloshin S A 1998 *Phys. Rev. C* **58** 1671
- [47] Bilandzic A, Snellings R and Voloshin S A 2011 *Phys. Rev. C* **83** 044913
- [48] Back B B *et al.* 2005 *Phys. Rev. C* **72** 051901
- [49] Kolb P F 2003 *Phys. Rev. C* **68** 031902(R)
- [50] Borghini N and Ollitrault J Y 2006 *Phys. Lett. B* **642** 227
- [51] Gong X Y *et al.* 2011 *J. Phys. G* **38** 124146
- [52] Bai Y *et al.* 2007 *J. Phys. G* **34** S903
- [53] Chen L W, Ko C M and Lin Z W 2004 *Phys. Rev. C* **69** 031901
- [54] Xu J and Ko C M 2011 *Phys. Rev. C* **84** 014903
- [55] Schenke B, Jeon S and Gale C 2011 *Phys. Rev. Lett.* **106** 042301
- [56] Teaney D and Yan L 2011 *Phys. Rev. C* **83** 064904
- [57] Luzum M, Gombeaud C and Ollitrault J Y 2010 *Phys. Rev. C* **81** 054910
- [58] Gardim F G, Grassi F, Hama Y, Luzum M and Ollitrault J Y 2011 *Phys. Rev. C* **83** 064901